



## Impact of two particle measurement techniques on the determination of N95 class respirator filtration performance against ultrafine particles

Reza Mostofi<sup>a</sup>, Alexandra Noël<sup>b</sup>, Fariborz Haghighat<sup>a,\*</sup>, Ali Bahloul<sup>c</sup>, Jaime Lara<sup>b</sup>, Yves Cloutier<sup>c</sup>

<sup>a</sup> Department of Building, Civil and Environmental Engineering Concordia University, Montreal, Quebec, Canada

<sup>b</sup> Department of Environmental and Occupational Health, University of Montreal, Montreal, Quebec, Canada

<sup>c</sup> Institut de Recherche Robert-Sauvé en Santé et en Sécurité du Travail, Montréal, Québec H3A 3C2, Canada

### ARTICLE INFO

#### Article history:

Received 27 October 2011

Received in revised form 21 February 2012

Accepted 22 February 2012

Available online 2 March 2012

#### Keywords:

N95 filtering facepiece respirator

Ultrafine particles

Penetration

Poly disperse aerosols

Penetrating particle size

### ABSTRACT

The purpose of this experimental study was to compare two different particle measurement devices; an Electrical Low Pressure Impactor (ELPI) and a Scanning Mobility Particle Sizer (SMPS), to measure the number concentration and the size distribution of NaCl salt aerosols to determine the collection efficiency of filtering respirators against poly disperse aerosols. Tests were performed on NIOSH approved N95 filtering face-piece respirators (FFR), sealed on a manikin head. Ultrafine particles found in the aerosols were also collected and observed by transmission electron microscopy (TEM). According to the results, there is a systematic difference for the particle size distribution measured by the SMPS and the ELPI. It is largely attributed to the difference in the measurement techniques. However, in spite of these discrepancies, reasonably similar trends were found for the number concentration with both measuring instruments. The particle penetration, calculated based on mobility and aerodynamic diameters, never exceeded 5% for any size range measured at constant flow rate of 85 L/min. Also, the most penetrating particle size (MPPS), with the lowest filtration efficiency, would occur at a similar ultrafine size range <100 nm. With the ELPI, the MPPS was at 70 nm aerodynamic diameter, whereas it occurred at 40 nm mobility diameter with the SMPS.

© 2012 Elsevier B.V. All rights reserved.

### 1. Introduction

According to the Bureau of Labor Statistics and the National Institute for Occupational Safety and Health (NIOSH), in the USA in 2003, approximately 3.3 million workers in the private sector used a respirator to reduce workplace exposures [1]. With the exponential growth of nanotechnology and the potential impact of nano-materials on workers' health and safety, air filtration respirators are increasingly being used to reduce exposure to airborne nano-materials, when other control methods are insufficient. A recent research work has shown that elastomeric half-mask air purifying respirators are the most commonly used type of respirator worn by workers handling nanomaterials, followed by disposable filtering facepiece respirators (FFR) [2].

Workers could be exposed to nanoparticles during the manufacture of different nanotechnology related products or to ultrafine particles as incidental by-products of combustion or welding processes. Both types of particles have diameters smaller than 100 nm, and this could potentially pose a health hazard [3]. Epidemiological studies on exposures to ultrafine particles, which are in the

same size range as nanoparticles, have clearly shown acute and chronic effects [4]. Also, toxicity studies on the effects of nanoparticles on animals have also shown acute effects on different organs; however, chronic studies are still very limited [5].

In order to understand and characterize toxicity of ultrafine particles, it is important to determine the particle characteristics from different views (i.e., mass concentration, number concentration, and size distribution). Various techniques have been developed to determine characteristics of the particles. However, most of these devices are not yet validated for ultrafine particle field and laboratory size measurements.

The effectiveness of filtering respirators and any other protective equipment to intercept and prevent ultrafine particles penetration is a significant issue that needs to be evaluated [6,7]. The distinctive lognormal particle size distribution curve is well known and documented experimentally and theoretically regarding filtration efficiency [7–9]. The lowest point of the curve is where the minimal collection efficiency was found and represents the range of most penetrating particle size (MPPS), which correspond to a median mass aerodynamic diameter of 350 nm for mechanical filters [7,8,10]. In general, for filters, particle sizes that approximate 50–500 nm are assumed to correspond to the range of MPPS [6,7,11]. According to their size, ultrafine particles (10–100 nm) principally respond to a diffusion mechanism, while

\* Corresponding author. Tel.: +1 514 848 2424x3192; fax: +1 514 848 7965.

E-mail address: [haghi@bcee.concordia.ca](mailto:haghi@bcee.concordia.ca) (F. Haghighat).

sub-micrometric particles (300–1000 nm) essentially respond to interception, impaction and gravitational settling mechanisms [7,11,12]. Previous experimental studies on the efficiency of different NIOSH certified filtering face-piece respirators with ultrafine particles using a constant flow rate of 85 L/min (or 42.5 L/min for dual filter respirators) to represent a worker's inhalation at heavy load burden, showed that the MPPS was at 200 nm or below [10,11]. The experimental approach used by NIOSH for filter approvals is described in the 42 CFR part 84, "Respiratory Protective Devices" [13]. The limitations of the NIOSH experimental set-up and protocol are well discussed by Eninger et al. [21]. The main limitation of this protocol is that it uses aerosol photometers that do not effectively detect the ultrafine aerosol fraction. Manikin-based experimental set-ups to characterize the respirator filter performance have been used in earlier studies and is described in details in the literature [14–21]. The results obtained with the various different methodologies including experimental set ups, aerosol size ranges and particle size measurement techniques that have been used in previous studies are not always directly comparable [10–12,14–22]. Since exposures to nanomaterial and ultrafine particles are increasing and that several ultrafine size measuring instruments are available, endeavours must be made in regards to the evaluation of filtering respirators initial penetration of ultrafine particles or their agglomerates that are within MPPS range [6]. For this reason, it is important the comparison of commonly used ultrafine size measuring techniques, to better understand their advantages and limitations.

Regarding penetration of ultrafine particles through the FFRs, in most of the previous studies, the Scanning Mobility Particle Sizer (SMPS) technique, comprised of Differential Mobility Analyzer (DMA) and Condensation Particle Counter (CPC), has been used to determine the particle number concentration and size distribution and consequently to calculate the filtration efficiency at each particle size range. The electrical low pressure impactor (ELPI) has been also used to measure the size of particles when assessing the evaluation of protection factors and filtering efficiency of NIOSH certified N95 FFR [10,18,19].

In this study, two techniques to characterize the number concentration and size distribution of ultrafine particles have been employed to measure filter efficiency using a manikin-based experimental set-up [16–20] and the data have been compared. To our knowledge, no previous studies have investigated the use of different measuring techniques, mobility and impaction, to characterize the filtration efficiency of respirators.

The objective of this study was to compare two different particle measurement techniques, an Electrical Low Pressure Impactor (ELPI) and a Scanning Mobility Particle Sizer (SMPS), to measure the number concentration and the size distribution of salt aerosols in order to determine the collection efficiency of filtering respirators.

## 2. Instrumentation

Concerning available measurement techniques, the ELPI and the SMPS are devices currently used to determine the particle size distribution of aerosols in the ultrafine size range (1–100 nm). The measurement done by each device has its own principle and technique. With the ELPI, the particles are size classified based on inertia impaction, while for the SMPS, the electrical mobility is behind the measurement. Compared with the SMPS, the ELPI measures the particles over a wider size range. Based on the aerodynamic diameter, particles are segregated onto 12 different cut-off diameters, ranging from 30 nm to 10  $\mu\text{m}$ , each corresponding to a specific impactor stage. The resolution of the size distribution of the ELPI measured through 12 different stages is lower than that of the SMPS measured through 167 different channels. Nonetheless, the ELPI has the advantage of having a high time resolution which allows

taking measurements of the entire size distribution simultaneously every second, whereas the SMPS, which operates on a scanning channel per channel basis, cannot [8,23]. However, for the SMPS, the particle size distribution measurements are done at high resolution, for size range between 5 and 1000 nm [24].

In the SMPS, to obtain the Boltzmann charge equilibrium, the particles are passed through a neutralizer before entering the main part of the SMPS; DMA. Then, the particles are selected in the DMA according to their electrical mobility. As the particles enter the DMA, they experience an external electric field causing each particle with a certain diameter and charge to follow a specific trajectory, and to migrate with a certain amount of velocity. Only specific size-selected particles within a narrow range of electrical mobility will have the correct trajectory to exit the DMA. Particle size distributions are established by changing the voltage between the inner and outer cylindrical electrodes in the DMA, which changes the electrical field. DMA voltage ( $V$ ) is related to the electrical mobility,  $Z$ , and mobility diameter,  $d$ , using Eq. (1):

$$Z = \frac{Q \ln(R_2/R_1)}{2\pi LV} = \frac{0.441(k_B T/M)^{0.5}}{pd^2} \quad (1)$$

where  $R_1$  and  $R_2$  are the inner and outer radius of the DMA,  $L$  is the DMA length from inlet to outlet slit,  $Q$  is the carrier gas flow rate,  $k$  is the Boltzmann constant, and  $T$ ,  $p$ , and  $M$  are the temperature, pressure and molecular weight of the carrier gas [25]. In the second part of SMPS, a CPC then optically detects and counts these particles.

In the ELPI, particles first pass through a corona charger, where they are positively charged. Then, to classify the particles in terms of their inertia impaction and aerodynamic diameter, the charged particles go through a cascade impactor which consists of 12 different stages. The large particles unable to follow the stream are collected on the upper stages and the smaller ones follow the stream and are impacted on the proper-lower stages. Once any positively charged particle is collected at any stage, an electrical current carried by the particle is counted by an electrometer. Finally, the counted current measured at any stage is related to the number concentration by applying Eq. (2):

$$C_i = \frac{I}{PneQ} \quad (2)$$

where  $C_i$  is the number concentration of the particle,  $I$  is the induced current,  $P$  is the particle penetration through the corona charger,  $n$  is the number of the charges carried by the particle,  $e$  is the charge of an electron ( $1.602 \times 10^{-19}$ ) and  $Q$  is the sampling flow rate [26].

In this study, the ELPI (Dekati Ltd., Tampere, Finland) was operated at a flow rate of 10 L/min and was employed using the standard configuration for the 12 stage cascade impactor. Oiled sintered impaction substrates, to prevent or reduce particle bounce and re-entrainment, were placed in the impactor. The particle density used for the measurements was set at 2.17 g/cm<sup>3</sup>, as this is the value of NaCl bulk density. In addition, all the data provided with the ELPI was reported based on the particle collection diameter ( $Di_n$ ), which is referred to as the midpoint value between the cut-off diameter of the given stage ( $Da_n$ ) and the cut-off diameter of the stage located above ( $Da_{n+1}$ ). This was calculated using Eq. (3):

$$Di_n = \sqrt{(Da_n * Da_{n+1})} \quad (3)$$

## 3. Materials and methods

In this study, NIOSH approved N95 FFR from 3 M, model 8210 were selected to challenge against NaCl salt ultrafine particles. A detailed description of the manikin set-up has previously been published [27]. In summary, for each test, a selected N95 FFR was fixed on a manikin's face using a silicon sealant to avoid any possible



Fig. 1. Manikin head with the sealed N95 FFR in the challenge chamber.

leakage: the manikin was then placed inside the test chamber as shown in Fig. 1.

### 3.1. Experimental set-up

#### 3.1.1. Poly-dispersed aerosols filtration test (PAT)

Fig. 2 is a schematic representation of the experimental set-up used to characterize the filtration performance of the N95 FFRs against poly-dispersed sodium chloride particles. In this set-up, a six-Jet Collision Nebulizer (Model CN25, BGI Inc., Waltham, MA) was employed to generate poly-dispersed sodium chloride particles in the ultrafine size range (1–100 nm). A diffusion dryer (a silica gel drying system) was used to dry the aerosols coming out from the Collision Nebulizer. The particles were then passed through a neutralizer (Kr-85) (Model 3012A, TSI Inc.) to obtain the Boltzmann charge equilibrium and then it was mixed with dry air. The total aerosol stream at a constant flow rate of 85 L/min was passed directly into the test chamber. Further details on the experimental set-up, measurement techniques and procedure can be found in [27].

The particle penetration through the filter is determined as the ratio of the downstream concentration ( $C_{down}$ ) to upstream concentration ( $C_{up}$ ) for the challenge aerosol, which is presented in Eq. (4):

$$P(\%) = \left( \frac{C_{down}}{C_{up}} \right) \times 100 \quad (4)$$

Consequently, the total collection efficiency ( $\eta$ ) is defined in Eq. (5) as:

$$\eta(\%) = \left( \frac{C_{up} - C_{down}}{C_{up}} \right) \times 100 = 100 - P \quad (5)$$

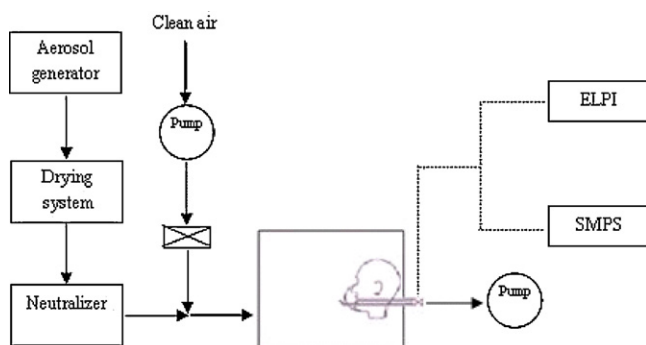


Fig. 2. Schematic diagram of the experimental set-up for testing N95 FFR against salt poly-dispersed aerosols using ELPI and SMPS measuring techniques.

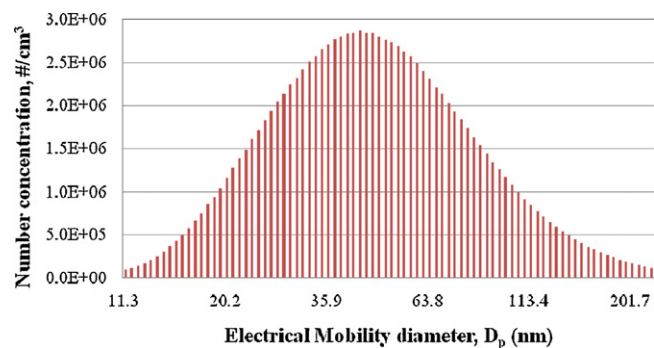


Fig. 3. Particle concentration and size distribution of the challenge NaCl aerosols upstream at 85 L/min testing flow rate using the SMPS measuring technique ( $n=4$ ).

The concentration (of whether upstream or downstream) applied in above formulas is number concentration based, which is defined as  $C_i$  for the ELPI (see Eq. (2)) and as the total number counted by CPC divided by the volume of air for the SMPS device.

The sampling flow rates were of 1.5 and 10 L/min respectively for SMPS and ELPI measure techniques. After stabilization of the system, the size distribution were measured alternately twice at the downstream and upstream of the test filter with both SMPS and ELPI. Each ELPI measurement was recorded for 2 min and 15 s, which corresponded approximately to the time needed by the SMPS to perform a total particle size scan. The particle penetrations were determined as function of mobility and aerodynamic particle sizes using SMPS and ELPI as the measuring techniques, respectively.

### 3.2. Generation of poly-dispersed sodium chloride particles

A six-Jet Collision Nebulizer was operated at an inlet pressure of 25 psi, and fed with 0.1% (v/v) NaCl solution to generate poly-dispersed NaCl particle (see Fig. 3). Prior to a filtration efficiency test, the generation system was allowed to operate for at least 5 min in order to reach a steady state condition. To reduce the chance of particle loading, the N95 FFR was bypassed during the stabilization period.

### 3.3. Transmission electron microscopy characterization of poly-dispersed sodium chloride particle

Aerosol sampling was performed for poly-dispersed sodium chloride particle characterization (optical size, shape and structure) by TEM (Philips CM200 equipped with a digital camera-Corel Corp. AMTV600 2Kx2K, 80 kV). A cassette fitted with a polycarbonate substrate and a TEM pre-metallized copper grid placed directly in the cassette was used to sample at a flow rate of 1 L/min for 10 min. The cassette was placed in front of the respirator. After sampling, the particles collected on the TEM pre-metallized copper grids placed in the cassette were analyzed directly by TEM without subsequent manipulation.

## 4. Results and discussion

### 4.1. Phase 1: particle size distribution and number concentration

In this experiment, the particle number concentration and size distribution at upstream of the filter, simultaneously measured with both SMPS and ELPI (particle density assumed =  $2.17 \text{ g/cm}^3$ ), were determined, as shown in Figs. 3 and 4.

Various ultrafine particle size measurement techniques exist based on distinct physical principles [28]. In this study, two techniques were used, namely differential mobility analysis and impaction. Microscopy offers valuable information regarding the

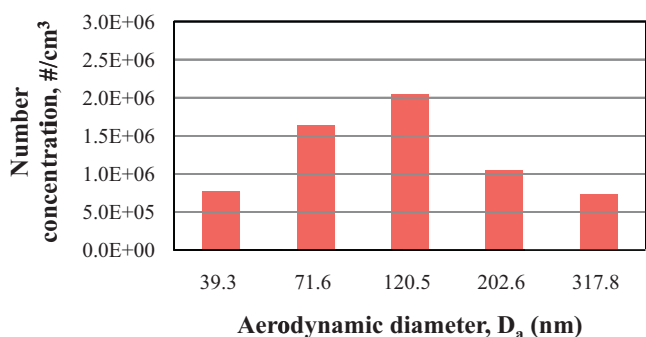


**Fig. 4.** Particle concentration and size distribution of the challenge NaCl aerosols upstream at 85 L/min testing flow rate using the ELPI measuring technique ( $n=4$ ).

morphology, and structure of particles. These three techniques are complementary and all relevant to characterization of airborne ultrafine particles [28]. Taken together, they can give a representative image of the exposure. However, results obtained by these different techniques are not directly comparable because they are based on different operating principles [28]. The essential difference in the operating principles of the ELPI and SMPS devices is that they both measure particle size but express it with different types of equivalent diameters: aerodynamic and electrical mobility, respectively [29]. For comparison purposes of these two devices, only the data of ELPI's stages 1–5 (mid-point from 39.3 to 317.8 nm) were taken, since this size measurement range overlapped with the SMPS. Measuring number concentrations with various devices, which have distinct lower and upper bound size sensibility, may give different results [23]. Therefore, interpretations of aerosols characteristics measured with different techniques must integrate the advantages and disadvantages related to each device, including the limits of detection [30]. The ELPI has a size resolution of 30–10,000 nm, a time resolution of 2–3 s and a limit of detection for particle concentration that is dependant on particle size [26]. Lower and upper limits of detection for number concentration are 142 and  $3.8 \times 10^7/\text{cm}^3$ , respectively, for the lowest stage (stage 1) and for stage #5, 5 and  $1.4 \times 10^6/\text{cm}^3$  [26]. As shown in Fig. 4, results were always within the lower and upper detection limits of the ELPI. The detection limits of the SMPS is, in terms of particle diameter, between  $d_{\text{sph}} = 10$  nm and  $1 \mu\text{m}$ .

Consequently, when comparing the results obtained with the SMPS and the ELPI, there seems to be a systematic difference for the particle size distribution measured by the two instruments, mainly attributed to the difference in measurement techniques and the way of displaying the results. As observed in Figs. 3 and 4, the trend for the number concentration measured by the SMPS and ELPI displayed a similarity. The plots of ELPI and SMPS results show that number concentration and size distribution measured by the ELPI and the SMPS follow similar trend, although the number concentration seems slightly higher with the SMPS and the particle size distribution lightly shifts to larger particles with the ELPI.

It must be kept in mind that the SMPS could possibly modify the aerosol since it intercepts large particles by a pre-impactor prior to the analyzer [31]. In this way, SMPS could brake large aerosol agglomerates, resulting in a higher count of smaller particles or agglomerates and thus, a slightly bias measurement towards smaller sizes [31]. Also, the higher number concentration measured by the SMPS could possibly be explained by the fact that this device has a lower detection bound of 5 nm and 78 channels in the ultrafine size range. According to this device, the aerosol sampled was composed, among others, of ultrafine particles or ultrafine particle agglomerates ranging between 5 and 30 nm (see Figs. 3 and 7). This specific size range is too small to be size segregated by the ELPI having a lower detection bound of 30 nm and only two stages

below 100 nm. The particle size distribution could not be displayed at high resolution in the ultrafine size range (1–100 nm) with the ELPI. Therefore, the SMPS has the capability of detecting smaller ultrafine particles (<30 nm) than the ELPI and consequently, counting a higher number of total particles if small ultrafine particles (<30 nm) are present in the aerosol. Based on their respective operating principles, we observed a shift of the SMPS size distribution to smaller diameters and thus, there was a gap between the size distributions measured by these two devices, illustrating the two distinct type of size characterization [29,32].

Our results are in accordance with other studies that used these two devices to characterize ultrafine particle size and number concentration in aerosols. In a study conducted by Rossi et al., [33], they used simultaneously an ELPI and a SMPS to characterize aerosols composed of  $\text{TiO}_2$  and  $\text{SiO}_2$  nanoparticles. Their results showed that systematically, the number concentration measured by the SMPS was slightly higher than the one reported by the ELPI, whereas the size distribution, reported by a  $D_{50}$  value, was vaguely smaller for measurements made with the SMPS when compared to values measured by the ELPI [33]. Comparison of measured particle size distributions made with a SMPS and an ELPI was also performed in a study conducted by Marjamaki et al. [34]. They showed that there was a reasonably good agreement between the size distributions measured by these two devices [34]. These data and the results of our study also suggest that the aerodynamic diameter ( $D_a$ ) would be larger than the electrical mobility diameter ( $D_p$ ). Overall, comparison of the analysis shows good agreement, but SMPS provides additional information regarding number concentration in the lower ultrafine size range (<30 nm).

Noteworthy, assuming a unique density for the particles collected on each stage of the ELPI, is another potential factor which may cause a discrepancy in the measured particle number concentration when comparing with the results obtained with the SMPS. According to Marjamaki et al. [34], this assumption may bring some inaccuracy (as high as 100%) in determining the particle number concentration collected on each stage since the particle density may change with particle size and thus, from one stage to another, supported by the fact that we have generated poly-dispersed aerosols [35]. Furthermore, some of the particles observed by TEM were agglomerated and not perfectly spherical, shape seemed more cuboidal (Figs. 7 and 8). Particles of different shape and agglomeration state will have a density that will vary accordingly and as mentioned above, this can influence the ELPI size measurement.

The mobility diameter measured with the SMPS is close to being comparable to the projected-area diameter of particles, which can be observed and measured by TEM [23]. Therefore, particle size measurements made by SMPS and by TEM could lead to an advantage that the obtained results can be compared without any additional suppositions regarding particles shape and/or density. While such information could be complex to determine and is fundamental when comparing results obtained with cascade impactors and TEM [23].

#### 4.2. Phase 2: filtering respirators initial particle penetration against ultrafine NaCl particles

The N95 FFR were challenged with poly-dispersed NaCl aerosols for a period of 5 min at 85 L/min constant flow rate, and characterization was done simultaneously using both the SMPS and the ELPI instruments. The test was repeated four times. The mean, peak and standard deviation of initial penetration values were computed with respect to the electrical mobility diameter and the aerodynamic diameter, measuring particle size distribution and number concentration at upstream and downstream with the SMPS and the ELPI, respectively. The number of replicates in this study ( $n=4$ ) showed that results were fairly constant from one test to



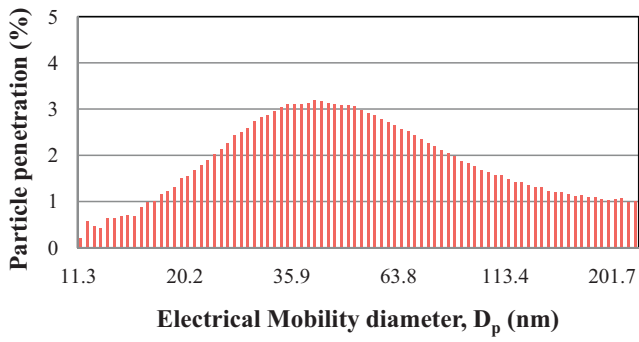


**Fig. 5.** N95 respirators initial particle penetration as a function of particle diameter at 85 L/min flow rate using the SMPS measuring technique ( $n=4$ ).

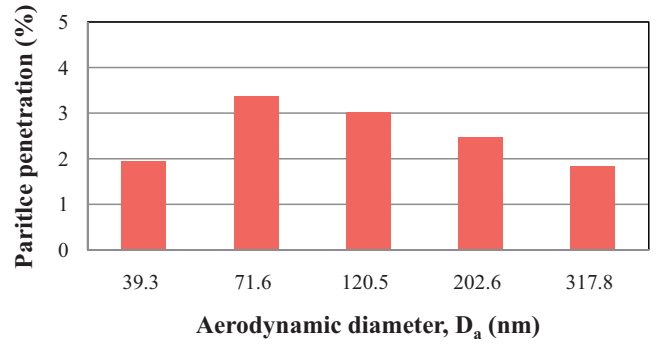


**Fig. 6.** N95 respirators initial particle penetration as a function of particle diameter at 85 L/min flow rate using the ELPI measuring technique ( $n=4$ ).

another. For all 4 masks tested, the mean average penetration was  $1.78 \pm 0.83\%$  for a size distribution ranging from 11 to 225 nm measured on 83 different channels of the SMPS and was of  $2.47 \pm 0.66\%$  for sizes ranging from 39 to 318 nm measured on 5 stages of the

ELPI. Figs. 5 and 6 show the initial particle penetration values. Although the measurement techniques used by each device are different, as illustrated in Figs. 5 and 6 at their MPPS, the maximum initial penetration level measured with the SMPS was in agreement

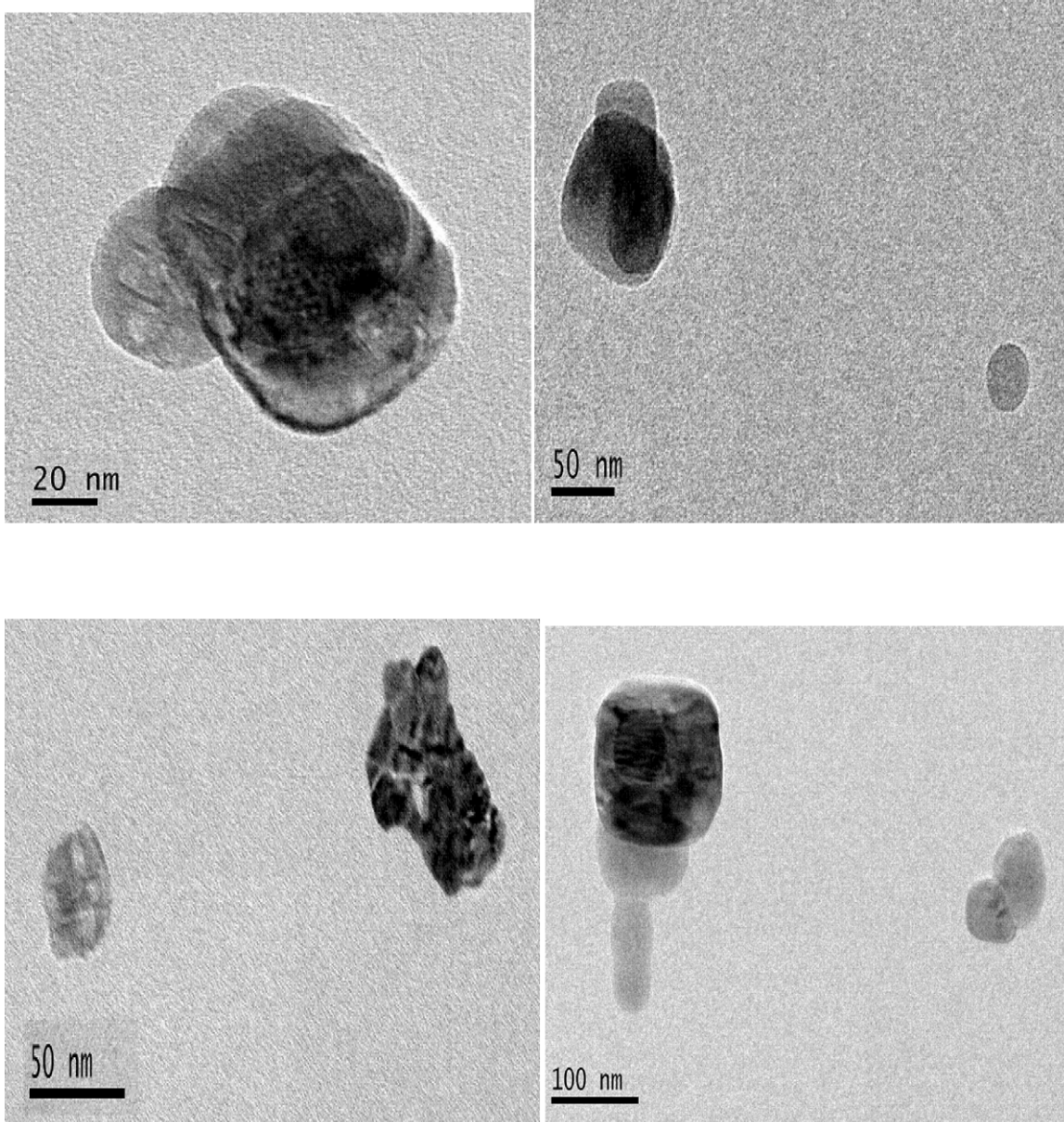


**Fig. 7.** TEM images of poly-dispersed NaCl in aerosol.

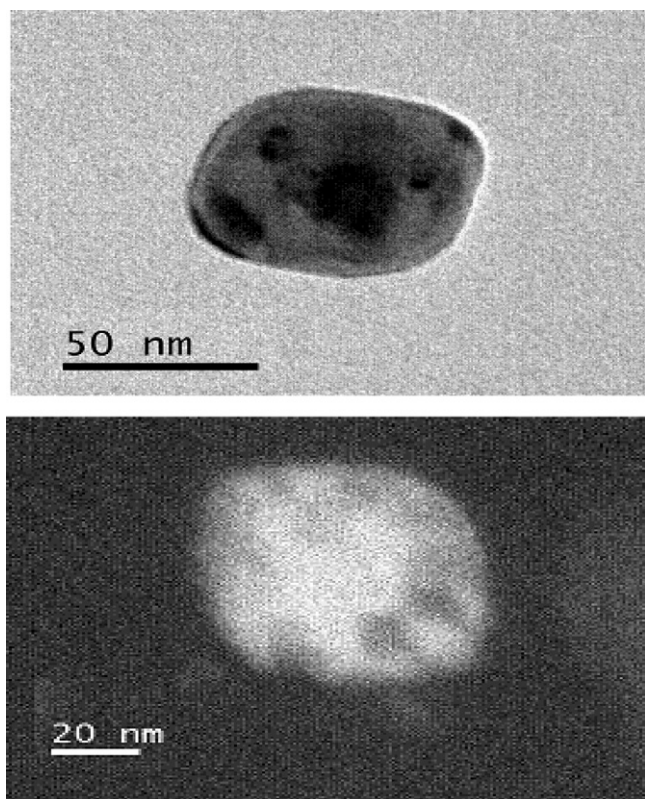


Fig. 8. TEM images of NaCl particles in aerosol.

with the maximum initial penetration measured with the ELPI. As illustrated in Figs. 5 and 6, the plots of ELPI and SMPS results for the FFR N95 respirators average initial penetration measured by these two devices follow a similar trend. The maximum initial penetration values were of 3.08 (standard deviation of 0.10) and 3.37 (standard deviation of 0.12) when particle concentration was counted by SMPS or the ELPI, respectively. Also the MPPS occurred at 70 nm aerodynamic diameter with the ELPI and 40 nm mobility diameter with the SMPS. Noteworthy, these MPPS values should be unequal, since they are based on two different units, one is the electrical mobility diameter measured with an SMPS and the other one is the aerodynamic diameter determined by impaction. By correlating these two units, similar values should theoretically be obtained. However some other parameters such as, particle density and shape for each particle size, are required for such correlation and the true values of these parameters are unknown (see Figs. 7 and 8) and therefore, were not computed. Nonetheless, in both cases (ELPI and SMPS), the lowest filtration efficiency measured by the MPPS, would occur at a similar ultrafine size range (<100 nm), acknowledging the presence of electrostatic attraction mechanism on the filter particle collection. This is in accordance with what has been previously reported [11,16,36]. In our study, in both cases, using either the electrical mobility or the aerodynamic diameter, the initial penetration did not exceed the 5% NIOSH certification criterion at 85 L/min of the FFR N95 class respirator. Some studies [16–36] presented penetration values at MPPS below 5% for some NIOSH-certified filtration respirators and at the same time, borderline values or exceeding 5%, thus, highlighting the need for harmonization of protocols and the need of performing more research in this particular field.

As observed in Fig. 5, with the SMPS, for particles between 40 and 202 nm in electrical mobility diameter, the mean particle penetrations varied from 3.08 to 0.97%, showing a reduction by an average factor of 3.18 for the lower tail of the particle size

distribution (<40 nm). In Fig. 6, for the 5 stages evaluated with the ELPI, the mean particle penetrations varied from 3.3 to 1.9%, showing a reduction by an average factor of 1.74 for the lower tail of the particle size distribution (<72 nm). The results of this study support the validation of FFR N95 filter efficiency certification for these respirators against NaCl ultrafine salt particles for the size range that was used.

Images obtained by TEM of poly-dispersed NaCl ultrafine particles in aerosol are showed in Figs. 7 and 8. Primary particles seemed cuboidal. As we can observe, the optical size of NaCl particles seems to vary but remain in the ultrafine size range (<100 nm), with the presence of agglomerates that can exceed 100 nm. We also noticed that NaCl particles or agglomerates of particles had different shape and structure (Figs. 7 and 8). Therefore, images obtained by TEM qualitatively support the results obtained by the two different measuring techniques, that is to say NaCl particles generated in aerosol were mainly ultrafine. Nonetheless, we must be cautious about the results obtained by microscopy, since we have sampled salt ultrafine particles, which can produce artifacts when drying into crystal or films onto the substrate, resulting in changes of shape and structure [28].

## 5. Conclusions

In this study, two distinct size measuring techniques, impaction and electrical mobility, were used to document the efficiency of filtration respirators for airborne ultrafine particles protection, which allowed characterization of number concentration and particle size distribution for salt aerosols. This type of characterization, added to analysis of TEM images, contributes to enhance our comprehension and provides useful information regarding aerosols characteristics that can influence the determination of respirators filtration performance. The results of this study demonstrated a similar trend for the filtration performance of a NIOSH approved filtering face-piece N95 FFR from 3M, model 8210, measured simultaneously with the SMPS and the ELPI instruments. The results also showed that, in both cases, the MPPS, with the lowest filtration efficiency, would occur at a similar ultrafine size range (<100 nm), acknowledging the presence of electrostatic attraction mechanism on the filter particle collection. With the ELPI, the MPPS was 70 nm aerodynamic diameter, whereas, the MPPS occurred at 40 nm mobility diameter with the SMPS. It should however be mentioned that the MPPS values should be unequal, since they are based on two different units, one is the electrical mobility diameter measured with an SMPS and the other one is the aerodynamic diameter determined by impaction.

Overall, in this study, the initial penetration never exceeded the 5% NIOSH certification criterion at 85 L/min for the FFR N95, reinforcing the fact that this level of filtration performance can be achieved for this type of respirator against ultrafine NaCl salt particles based on both electrical mobility and aerodynamic diameters.

## Acknowledgements

The authors would like to express their gratitude to the Institut de Recherche Robert-Sauvé en Santé et en Sécurité du Travail, Nano-Quebec and Concordia University for the financial support.

## References

- [1] National Institute for Occupational Safety and Health (NIOSH) and the Bureau of Labor Statistics (BLS), Respirator Usage in Private Sector Firms, Department of Health and Human Services & Department of Labor, 2003.
- [2] M.M. Dahm, M.S. Yencken, M.K. Schubaure-Berigan, Exposure Control Strategies in the Carbonaceous Nanomaterial Industry, *J. Occup. Environ. Med.* 53 (6) (2011) S68–S73.
- [3] National Institute for Occupational Safety and Health (NIOSH), Department of Health and Human Services, Centers for Disease Control and Prevention,



- Approaches to Safe Nanotechnology Managing the Health and Safety Concerns Associated with Engineered Nanomaterials, 2009.
- [4] H. Yang, C. Liu, D. Yang, H. Zhanga, Z. Xia, Comparative study of cytotoxicity, oxidative stress and genotoxicity induced by four typical nanomaterials: the role of particle size, shape and composition, *J. Appl. Toxicol.* 29 (2009) 69–78.
  - [5] C. Ostiguy, B. Soucy, G. Lapointe, C. Woods, L. Ménard, Les Effets Sur la Santé Reliés aux Nano-particules, 2nd édition, Rapport IRSST R-558, 2008.
  - [6] M.L. Ostraat, K.A. Swain, R.J. Small, Insight into the behavior of engineered aerosolized nanoparticles, *Int. J. Occup. Environ. Health* 16 (2010) 458–466.
  - [7] T. Schneider, D.H. Brouwer, I.K. Koponen, K.A. Jensen, W. Fransman, B. Van Duuren-Stuurman, M. Van Tongeren, E. Tielemans, Conceptual model for assessment of inhalation exposure to manufactured nanoparticles, *J. Expo. Sci. Environ. Epidemiol.* 21 (2011) 450–463.
  - [8] W.C. Hinds, *Aerosol Technology, Properties, Behavior and Measurement of Airborne Particles*, John Wiley & Sons Inc., New York, 1999, 483 pp.
  - [9] T. Ferge, J. Maguhn, H. Felber, R. Zimmermann, Particle collection efficiency and particle re-entrainment of an electrostatic precipitator in a sewage sludge incineration plant, *Environ. Sci. Technol.* 38 (2004) 1545–1553.
  - [10] S.A. Lee, S.A. Grinshpun, T. Reponen, Respiratory performance offered by N95 respirators and surgical masks: human subject evaluation with NaCl aerosol representing bacterial and viral particle size range, *Ann. Occup. Hyg.* 52 (2008) 177–185.
  - [11] R.E. Shaffer, S. Rengasamy, Respiratory protection against airborne nanoparticles: a review, *J. Nanopart. Res.* 11 (2009) 1661–1672.
  - [12] S. Rengasamy, W.P. King, B. Eimer, Filtration performance of NIOSH-approved N95 and P100 filtering-facepiece respirators against 4–30 nanometer size nanoparticles, *J. Occup. Environ. Hyg.* 5 (2008) 556–564.
  - [13] Respiratory Protective Devices, Code of Federal Regulations, Title 42, Part. 84, 1995, pp. 30355–30404.
  - [14] S. Rengasamy, B. Eimer, R.E. Shaffer, Comparison of nanoparticle filtration performance of NIOSH-approved and CE-marked particulate filtering facepiece respirators, *Ann. Occup. Hyg.* 53 (2009) 117–128.
  - [15] S. Rengasamy, A. Miller, B. Eimer, Evaluation of the filtration performance of NIOSH-approved N95 filtering facepiece respirators by photometric and number-based test methods, *J. Occup. Environ. Hyg.* 8 (2011) 23–30.
  - [16] A. Balazy, M. Toivola, T. Repoen, A. Podgorski, A. Zimmer, S.A. Grinshpun, Manikin-based performance evaluation of N95 filtering face-piece respirators challenged with nano-particles, *Ann. Occup. Hyg.* 50 (2006) 259–269.
  - [17] S.A. Lee, T. Reponen, W. Li, Development of a new method for measuring the protection provided by respirators against dust and microorganisms, *Aerosol Air Qual. Res.* 4 (2004) 55–72.
  - [18] B.U. Lee, M. Yermakov, S.A. Grinshpun, Unipolar ion emission enhances respiratory protection against fine and ultrafine particles, *J. Aerosol Sci.* 35 (2004) 1359–1368.
  - [19] B.U. Lee, M. Yermakov, S.A. Grinshpun, Filtering efficiency of N95- and R95-type facepiece respirators, dust-mist facepiece respirators, and surgical masks operating in unipolarly ionized indoor air environments, *Aerosol Air Qual. Res.* 5 (2005) 25–38.
  - [20] S.A. Lee, S.A. Grinshpun, A. Adhikari, Laboratory and field evaluation of a new personal sampling system for assessing the protection provided by the N95 filtering facepiece respirators against particles, *Ann. Occup. Hyg.* 49 (2005) 245–257.
  - [21] R.M. Eninger, T. Honda, A. Adhikari, H. Tanski, T. Reponen, S.A. Grinshpun, Filter performance of N99 and N95 face-piece respirators against viruses and ultrafine particles, *Ann. Occup. Hyg.* 52 (2008) 385–396.
  - [22] C.P. Schulte, C. Geraci, R. Zumwalde, M. Hoover, E. Kuempel, Occupational risk management of engineered nanoparticles, *J. Occup. Environ. Hyg.* 5 (2008) 239–249.
  - [23] A.D. Maynard, R.J. Aitken, Assessing exposure to airborne nanomaterials: current abilities and future requirements, *Nanotoxicology* 1 (2007) 26–41.
  - [24] TSI Product Information, 2000. [www.tsi.com/Particle/Product/Pisheets/3936/3936.htm](http://www.tsi.com/Particle/Product/Pisheets/3936/3936.htm) (accessed on February).
  - [25] J.F. De la Mora, L. De Juan, T. Eichler, J. Rosell, Differential mobility analysis of molecular ions and nanometer particles, *TrAC Trends Anal. Chem.* 17 (1998) 328–339.
  - [26] Dekati Ltd., *Electrical Low Pressure Impactor, User Manuel ver 4.0*, 2003.
  - [27] R. Mostofi, A. Bahloul, J. Lara, B. Wang, Y. Cloutier, F. Haghghat, Investigation of potential affecting factors on performance of N95 respirator, *J. Int. Soc. Resp. Protect.* 28 (2011) 26–39.
  - [28] K.W. Powers, M. Palazuelos, B.M. Moudgil, S.M. Roberts, Characterization of the size, shape and state of dispersion of nanoparticles for toxicological studies, *Nanotoxicology* 1 (2007) 42–51.
  - [29] D.H. Brouwer, J.H. Gijbbers, M.W. Lurvink, Personal exposure to ultrafine particles in the workplace: exploring sampling techniques and strategies, *Ann. Occup. Hyg.* 48 (2004) 439–453.
  - [30] D.B. Warheit, P.J.A. Borm, C. Hennes, J. Lademann, Testing strategies to establish the safety of nanomaterials: conclusion of an ECETOC workshop, *Inhal. Toxicol.* 19 (2007) 631–643.
  - [31] L.S. Ma-Hock, V. Burkhardt, A.O. Strauss, K. Gamer, Development of a short-term inhalation test in the rat using nano-titanium dioxide as a model substance, *Inhal. Toxicol.* 21 (2009) 102–118.
  - [32] J. Maguhn, E. Karg, A. Kettrup, R. Zimmermann, On-line analysis of the size distribution of fine and ultrafine aerosol particles in flue and stack gas of a municipal waste incineration plant: effects of dynamic process control measures and emission reduction devices, *Environ. Sci. Technol.* 37 (2003) 4761–4770.
  - [33] E.M. Rossi, L. Pylkkänen, A.J. Koivisto, M. Vippola, K.A. Jensen, M. Miettinen, K. Sirola, H. Nykäsenoja, P. Karisola, T. Stjernvall, E. Vanhala, M. Kiilunen, P. Pasanen, M. Mäkinen, K. Hämeri, J. Joutsensaari, T. Tuomi, J. Jokiniemi, H. Wolff, K. Savolainen, S. Matikainen, H. Alenius, Airway exposure to silica-coated TiO<sub>2</sub> nanoparticles induces pulmonary neutrophilia in mice, *Toxicol. Sci.* 113 (2010) 422–433.
  - [34] M. Marjamaki, J. Keskinen, D.R. Chen, D.Y.H. Pui, Performance evaluation of the electrical low-pressure impactor (ELPI), *J. Aerosol Sci.* 31 (2000) 249–261.
  - [35] N. Coudray, A. Dieterlen, E. Roth, G. Trouvé, Density measurement of fine aerosol fractions from wood combustion sources using ELPI distributions and image processing techniques, *Fuel* 88 (2009) 947–954.
  - [36] A. Balazy, M. Toivola, A. Adhikari, S.K. Sivasubramani, T. Reponen, S.A. Grinshpun, Do N95 respirators provide 95% protection level against airborne viruses, and how adequate are surgical masks? *Am. J. Infect. Control* 34 (2006) 51–57.